32nd URSI GASS, Montreal, 19-26 August 2017

Novel Circularly-Polarized Horn Antennas and Phase-less Characterization Methods for sub-mm-wave and Terahertz Communication and Sensing

Shubhendu Bhardwaj [(1)], Niru K. Nahar [(1)], and John L. Volakis [(1)]
Department of Electrical and Computer Engineering,
The Ohio State University

Abstract

In this work, we extend the circularly-polarized antenna technology to sub-mm-wave band using two key innovations. First, we develop septum-less circularly-polarized (CP) horn antennas that can be easily fabricated for upto terahertz frequencies. The design-method, optimization and fabricated porotype with 37% axial-ratio bandwidth and 18 dBi gain for 90-140 GHz band have been shown. Secondly, we develop phase-less gain characterization methods for the gain measurements of CP antennas in these bands. We show that the developed method provides accurate CP gain results with significantly reduced cost of set-up. The proposed method is demonstrated for WR-8 band gain and pattern measurements of the developed CP-horn antenna.

1. Introduction

Wireless communication in millimeter and terahertz bands is important for emerging 5G communication technologies [1, 2]. Applications ranging from short distance communication (including Internet of Things (IoT) related applications) to mm-wave-communications (28 GHz, 38 GHz, 71-86 GHz) rely on such systems. Antenna technology in these bands has become important due to limited power from sources and high propagation losses. Specifically, circularly-polarized antennas are useful in communication systems where transmitter and receiver can have a relative rotation. Satellite-communication in 71-86 GHz band is an important application for such antennas.

In this work, we present two key innovations in the field of circularly polarized high gain antennas for sub-mm-wave / terahertz communication. First, we propose a new hexagonal waveguide based horn antenna that is fabrication friendly, and thus allows scaling of CP-horns to these frequencies. Secondly, we propose novel reflection based method for gain characterization of CP antennas. The proposed method is phase-less and does not require antenna rotation, and is thus significantly cost-effective and accurate for sub-mm-wave and terahertz bands. Using the presented method, we present one of the first CP gain and pattern measurements beyond 100 GHz.

In the following sections, we will present the theory, design-optimization, fabrication-details and measurement-results for the developed CP-horn in WR-8 band (90-140 GHz). We further present the phase-less measurement method and its application for the measurement of the developed CP horn. Note that the proposed measurement method was introduced as a tool for broadside CP gain measurement in [3]. In this work, we report on its application for CP pattern-measurements, while also testing its repeatability and precision.

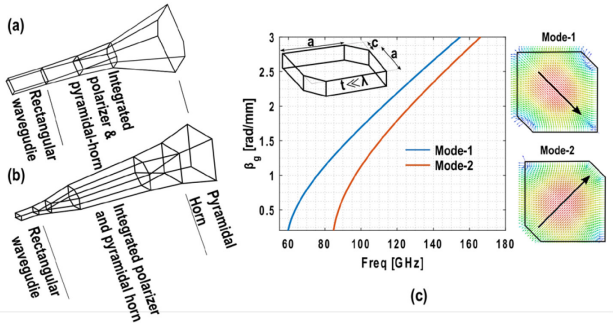

Fig. 1: Schematic of the proposed CP-horn antennas for sub-mm-wave/terahertz applications (a) low-gain horn design (c) high-gain horn design (c) dispersion relation within the hexagonal waveguides.

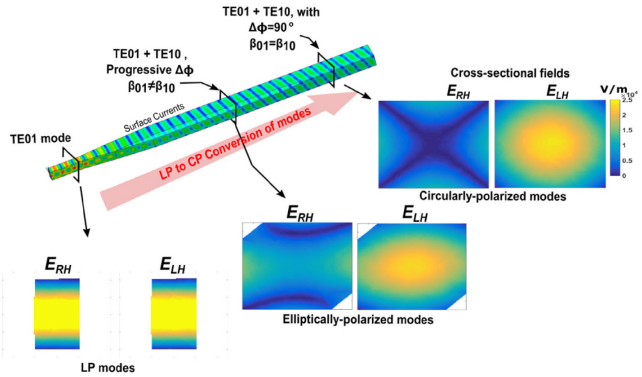

Fig. 2: Surface currents and cross-sectional fields showing evolution of CP modes in a waveguide at 110 GHz for a WR-8 band dimensions

2. Hexagonal Waveguide Based CP Horn Designs:

A number of CP antenna configurations have been proposed for sub-mm-wave and terahertz bands. Even so, due to complexity in design-structure and expensive fabrication-steps [4-9], a horn antenna remains attractive solutions for aforementioned applications. Even with these advantages, traditional CP-horns cannot be fabricated for sub-mm-wave/terahertz frequencies. This is because they employ a stepped partition within the waveguide (also known as stepped-septum horn [10]), which is difficult to be fabricated. We propose a class of horn antennas that

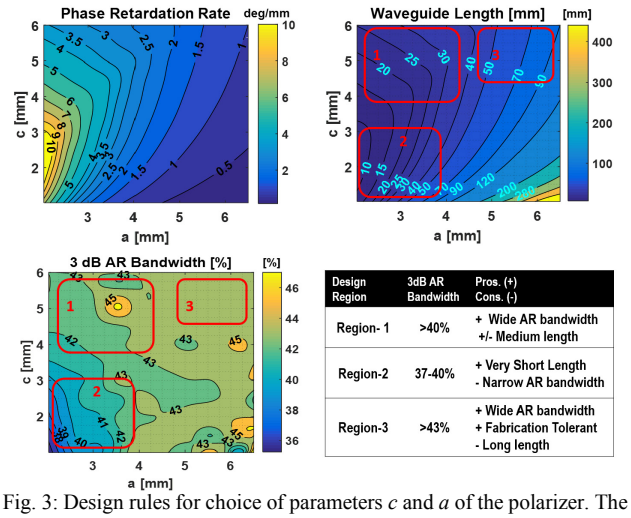

Design Region	3dB AR Bandwidth	Pros. (+) Cons. (-)
Region- 1	>40%	+ Wide AR bandwidth +/- Medium length
Region-2	37-40%	+ Very Short Length - Narrow AR bandwidth
Region-3	>43%	+ Wide AR bandwidth + Fabrication Tolerant - Long length

Fig. 3: Design rules for choice of parameters *c* and *a* of the polarizer. The choice depends on the required axial-ratio bandwidth and the size of the polarizer. Based on these, several recommended design choices are listed in the table.

avoid these partitions and are based on hollow waveguides (Fig. 1(a)-(b)). The designs exploit the dispersion properties in hexagonal waveguides for LP to CP conversion, leading to fabrication-friendly designs for terahertz operation.

2.1 Wave-Propagation in Hexagonal Waveguide:

A hexagonal cross-sectional waveguide exhibits varying dispersion properties for orthogonal modes (Fig. 1(c)) - a property we employ for conversion of linear polarized (LP) modes to Circularly-polarized (CP). Operation of such a waveguide for 110 GHz is illustrated in Fig. 2. As shown, we used TE_{01} input waveguide having a cross-sectional area of 2.032 mm × 1.016 mm, flared out to a square cross-section of area 2.032 mm × 2.032 mm and then to a hexagonal cross-sectional waveguide with a=2.032 mm, c=0.5 mm (parameters a and c are defined in Fig. 1(c)). Due to differential dispersion of orthogonal propagating-modes, a phase-lag is developed between them. The waveguide length and cross-section are optimized to obtain a 90° phase-lag at the end of the hexagonal section. After this, the waveguide is transitioned back to a square cross-sectional waveguide, causing the two modes to have identical phase-constant. Any further phase-lag is thus prohibited and the obtained polarization is maintained thereafter. We observe that this process allows right-hand (RH) to left-hand (LH) mode isolation of 40 dB, signifying high polarization purity of the output wave.

From a practical standpoint, we also desire polarizers to be 1) small in length and 2) have polarization purity in a wide frequency band. Therefore, we further study influence of cross-sectional shape and size on the axial-ratio (AR) bandwidth and waveguide-length in Fig. 3. Various possible design choices are also shown in this figure. We conclude that a narrow waveguide (e.g. as considered in Fig. 2) exhibits a small AR-bandwidth. For improvements in bandwidth and compactness, the polarizers should be flared (tapered out), leading to designs shown in Fig. 1(a) and 1(b).

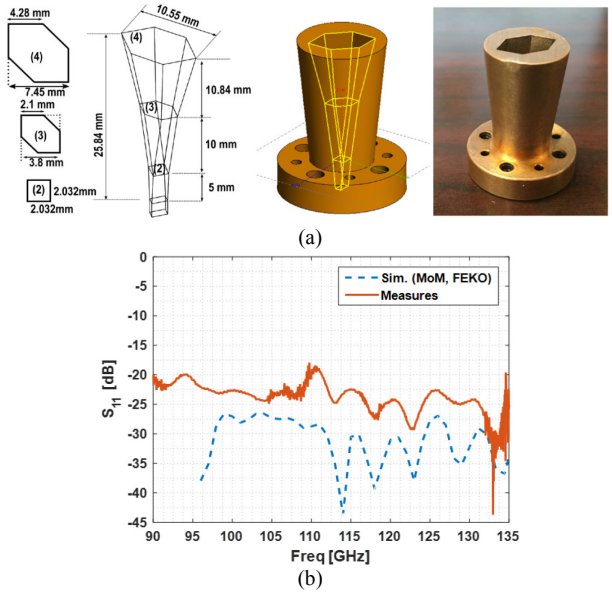

Fig. 4: (a) Schematic, 3D model and photograph of fabricated WR-8 band antenna using hexagonal CP horn concept (b) Measured and calculated reflection coefficient of the CP-horn prototype.

2.2 Sub-mm-wave prototype Development using the Proposed Design-Concept:

To demonstrate the CP horns using hexagonal waveguide concept, we fabricated and measured a prototype for WR-8 band (90-140 GHz) operation. The gain requirement for the objective design was 18 dBi, therefore, the low-gain design option (i.e., design shown in Fig. 1 (a)) was chosen. The design was optimized for low axial-ratio across the WR-8 band. The schematic and dimensions of the optimized design and a photo of the fabricated prototype is shown in Fig. 4. The measurement results for the prototype are reported in Sec. 4.

3. Hexagonal Waveguide Based CP Horn Designs:

In the proposed method, the AUT is used to measure the reflection from two standard scatterers: 1) a metallic dihedral corner reflector (DCR) and 2) a metallic plate. Fig. 5 shows these steps for broadside gain and pattern measurements. We note that due to its double reflection property, DCR reflects the power that is proportional to the co-pol gain of the AUT. On the other hand, for the metal plate, the reflected power is proportional to the product of the co-pol and cross-pol. Using image theory, it can be derived that the reflection-coefficients for the DCR and the metallic plate are [3]

$$|S_{11\{AUT\}}|^2_{DCR} = \frac{(G_{LH}^2 + G_{RH}^2)e_{prop}}{4\pi\left(\frac{2d_c}{\lambda}\right)^2} \quad (1)$$

$$|S_{11\{AUT\}}|^2_{plate} = \frac{4G_{RH}G_{LH}e_{prop}}{4\pi\left(\frac{2d_p}{\lambda}\right)^2} \quad (2)$$

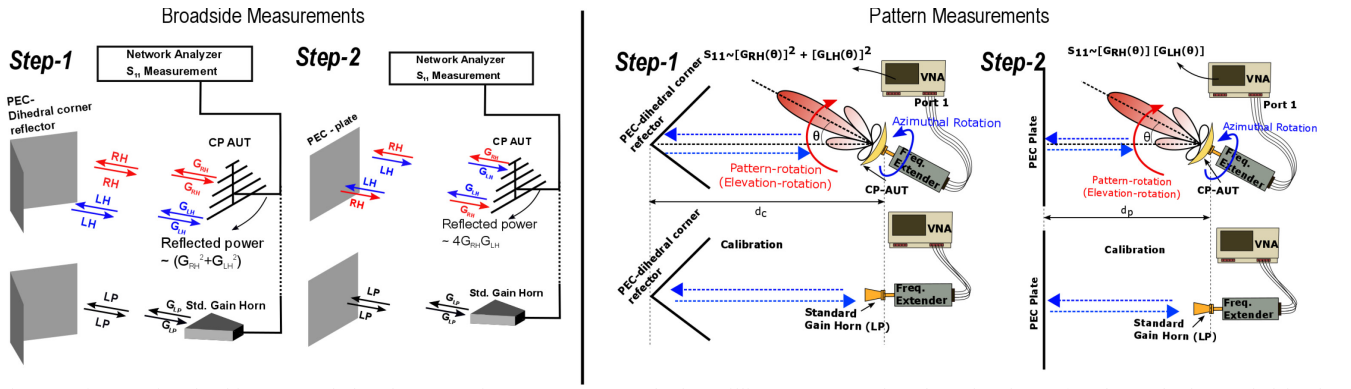

Fig. 5: *Left:* Steps involved in proposed phaseless CP-gain measurement method at millimeter wave and terahertz bands. *Right:* The method extended for the pattern-cut measurements of the AUT. As shown, the measurement steps remain identical with added AUT-rotation in the elevation plane.

In these, G_{RH} and G_{LH} are the RH and LH gains of the AUT, e_{prop} accounts for the atmospheric and reflection losses. Also, d_c is the distance between the AUT and the corner of the DCR, and d_p is that between the plate and the AUT. For reference, measurements are also carried out using a standard gain horn. Thus, we obtain $|S_{11\{horn\}}|^2_{DCR}$ and $|S_{11\{horn\}}|^2_{plate}$ respectively. Using these four parameters and knowing the gain of the horn (G_{horn}), variables e_{prop}, d_c and d_p can be eliminated from (1) and (2). Doing so, gives

$$G_{LH}^2 + G_{RH}^2 = \frac{|S_{11\{AUT\}}|^2_{DCR}}{|S_{11\{horn\}}|^2_{DCR}} G_{horn}^2 \quad (3)$$

$$4G_{RH}G_{LH} = \frac{|S_{11\{AUT\}}|^2_{plate}}{|S_{11\{horn\}}|^2_{plate}} G_{horn}^2 \quad (4)$$

As the right hand side of (3) and (4) are the extracted quantities from the measurements, we have two equations with two variables G_{RH} and G_{LH}. These can be solved to obtain the gain-characteristics of the AUT. Note that the process does not require phase-measurements and AUT-rotation and is robust to alignment errors.

4. Measurement Set-up and Measured Results:

4.1 Measurement Set-up:

Fig. 6 shows the measurement set-up for gain and pattern measurements. For our measurements, we used a corner reflector made of two square plates with side of 0.46 m (18″) (152λ at 100 GHz). The resulting corner-reflector had an aperture of 152λ × 215λ. One of the outer sides of the reflector was of size 152λ × 152λ and was used to form metal plate for the PEC-plate experiment. Notably, absorbers were used to avoid the specular reflections from the sides of the PEC-DCR and diffraction from the edges. To carry out the pattern-measurements, the AUT was scanned in the elevation-plane by rotating the frequency extenders, placed on a computer controlled turn-table. The used distances d_c and d_p (depicted in Fig. 5) were 0.56 m

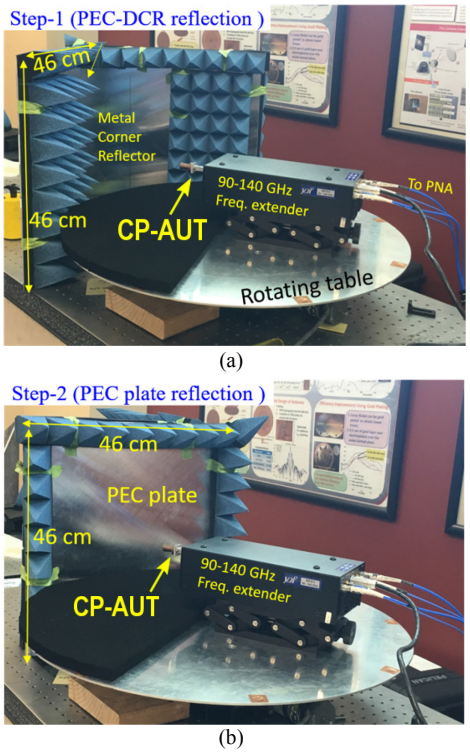

Figure 6: Measurement set-up used for the measurement of gain and patterns using the proposed phase-less gain measurement method (a) Step-1 of the proposed method (b) Step-2 of the proposed method.

(=22″) and 0.33 m (=13″), respectively. As shown in Fig. 5 and 6, RF cables in the back panel restricted the full-rotation of the turn-table. Therefore, the pattern measurements were only conducted with $\theta = \pm 25^o$ from the broadside of the AUT.

4.2 Measurement Results:

Broadside gain and pattern measurement results for the developed CP horn are presented in Fig. 7 and 8. We compare the simulation (FEKO, MoM) and measured results. We note that we expect a metal-overcut of ≈ 130 μm in the prototype, therefore simulations with overcut geometry are also shown. We find a good agreement between the simulations (with metal-overcut) and the measured data. Further, we use LP rotation method [10] to validate the proposed phaseless method for

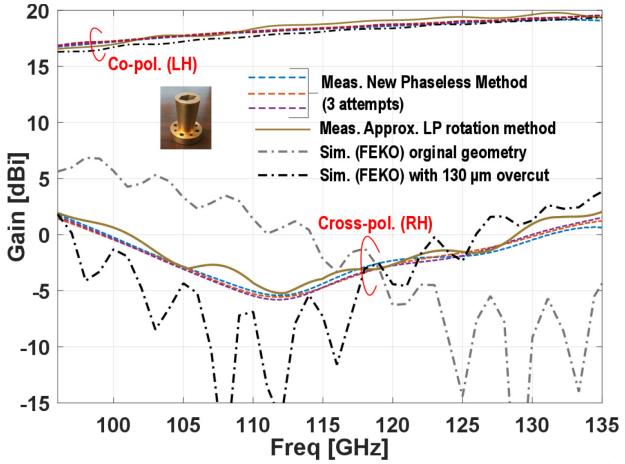

Fig 7: Measured co-pol. and cross-pol. gain (broadside direction) of the proposed hexagonal waveguide based horn prototype. Comparison with alternative measurement methods and calculations using full-wave simulations are also presented.

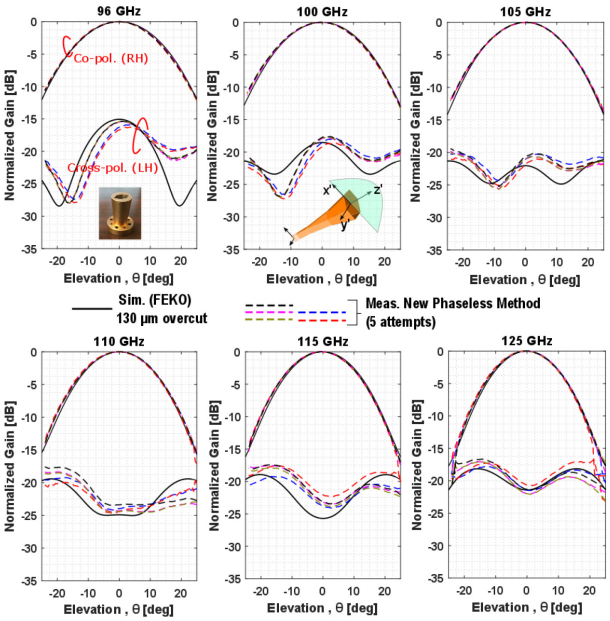

Fig. 8: Measured pattern-cut for the developed hexagonal CP-horn in its x'-z' plane (as shown in inset of second plot). Simulated (MoM, FEKO) and repeatability related data is also presented.

broadside direction. These further confirm the proposed method and the antenna operation.

Next, the simulated and measured pattern-cuts of co-polarized and cross-polarized gain are provided in Fig. 8. As shown, excellent accuracy is recorded for the co-pol and cross-pol patterns. Note that we have used the metal-overcut geometry simulations for these comparisons.

4.3 Uncertainty in the Measured Data:

Several measurement-samples (three to five) were taken to establish the repeatability tests for the proposed method. Average uncertainty (averaged over frequency and over three samples) in the broadside gain-measurements was found to be around 0.08 dB in co-pol and 0.28 dB in cross-pol. Equivalently, we estimated the average uncertainty in axial ratio to be 0.07 dB. The co-pol pattern measurements are also highly repeatable with an average uncertainty (standard deviation taken over 5 samples) of 0.10 dB. Whereas, cross-pol pattern measurements are repeatable within an uncertainty of 0.56 dB.

5. Conclusion:

In conclusion, we have presented two key technologies enabling the scaling of circularly-polarized antennas to sub-mm-wave and terahertz bands. Hexagonal waveguide concept has been used to design and optimize a hollow-waveguide based CP antenna. The developed prototype demonstrated a 37% axial ratio bandwidth. Further, phase-less measurement method for gain characterization of such antennas is presented. Specifically, it avoids the need for phase extraction of the received signals, eliminating the positioning errors in the measurements. It uses only a single-port measurements, implying elimination of one of the frequency extender units (as compared to traditional two-port methods). Using the proposed method, we showed one of the first CP-gain and pattern characterizations in waveguide-based sub-mm-wave bands.

6. References:

[1] T. S. Rappaport *et al*., "Millimeter Wave Mobile Communications for 5G Cellular: It Will Work!," in *IEEE Access*, vol. 1, no. , pp. 335-349, 2013.

[2] T. Kleine-Ostmann and T. Nagatsuma, "A Review on Terahertz Communications Research" in *Journal of Infrared, Millimeter, and Terahertz Waves,* vol. 32, no. 2, pp. 143–171, 2011

[3] S. Bhardwaj, N. K. Nahar, and J. L. Volakis, "Novel Phaseless Gain Characterization for Circularly Polarized Antennas at mm-wave and THz Frequencies," *IEEE Transactions on Antennas and Propagation*, vol. 63, no. 10, pp. 4263–4270, 2015.

[4] M. Euler, V. Fusco, R. Cahill and R. Dickie, "325 GHz Single Layer Sub-Millimeter Wave FSS Based Split Slot Ring Linear to Circular Polarization Convertor," in *IEEE Transactions on Antennas and Propagation*, vol. 58, no. 7, pp. 2457-2459, July 2010.

[5] X. Wu, G. V. Eleftheriades and T. E. van Deventer-Perkins, "Design and characterization of single- and multiple-beam mm-wave circularly polarized substrate lens antennas for wireless communications," in I*EEE Transactions on Microwave Theory and Techniques*, vol. 49, no. 3, pp. 431-441, Mar 2001.

[6] Y. M. Zhang et al., "Design of a Terahertz circularly polarized planar corrugated horn antenna," *Proceedings of 2014 3rd Asia-Pacific Conference on Antennas and Propagation*, Harbin, 2014, pp. 298-301.

[7] Y. Miura, J. Hirokawa, M. Ando, K. Igarashi and G. Yoshida, "A circularly-polarized aperture array antenna with a corporate-feed hollow-waveguide circuit in the 60 GHz-band," 2011 *IEEE International Symposium on Antennas and Propagation* (APSURSI), Spokane, WA, 2011, pp. 3029-3032.

[8] Hirokawa, J., Kim, D., Ando, M., Nagatsuma, T., Takeuchi, J., Hirata, A.: 'Wideband waveguide slot array antennas with corporate-feed in 120 GHz and 350 GHz bands'. *Proc. URSI Int. Symp. Electromagnetic Theory (EMTS)*, 2013, pp. 866–867

[9] S. Bhardwaj, N. K. Nahar and J. L. Volakis, "Radial line slot array antenna with vertical waveguide feed for F-band communication," in *IET Microwaves, Antennas & Propagation*, vol. 9, no. 3, pp. 193-199, 2 19 2015.

[10] D. Davis, O. Digiondomenico and J. Kempic, "A new type of circularly polarized antenna element," 1967 *Antennas and Propagation Society International Symposium*, Ann Arbor, MI, USA, 1967, pp. 26-33.

[11] IEEE Standard Test Procedures for Antennas, ANSI/IEEE 149, 1979 [Online].